Isotope-Engineered Single-Wall Carbon Nanotubes; A Key Material for Magnetic Studies

Mark H. Rümmeli,*,† Markus Löffler,† Christian Kramberger,† Ferenc Simon,§,|| Ferenc Fülöp,§ Oliver Jost,‡ Ronny Schönfelder,† Alexander Grüneis,† Thomas Gemming,† Wolfang Pompe,‡ Bernd Büchner,† and Thomas Pichler†

IFW Dresden, P.O. Box 270116, D-01171 Dresden, Germany, Dresden University of Technology, D-01062 Dresden, Germany, Budapest University of Technology and Economics, Budapest, P.O. Box 91, Hungary, and Vienna University, Strudlhofgasse 4, A-1090 Wien, Austria

Received: October 16, 2006; In Final Form: January 22, 2007

Common catalysts for single-wall carbon nanotube (SWCNT) synthesis have magnetic components, even after extensive purification. This prevents their use in key experimental studies such as nuclear magnetic resonance spectroscopy and studies on the as-yet unresolved question of superconductivity and encapsulated single-molecule magnets in SWCNTs. Thus, there is a pressing need for SWCNT samples with no foreign magnetic components. Experimental spectroscopic and microscopy findings confirm that we have directly synthesized high-quality isotope-engineered SWCNTs with controllable and well-defined narrow diameter distributions. Purities better than 70% are obtained with optimization. Additionally, novel isotope effects were observed. Electron spin resonance studies explicitly show magnetization levels below the instrument limits, and superconducting quantum interference device studies show no magnetic component. The obtained SWCNTs succesfully meet a broad set of criteria, making them highly suited to a variety of important studies that will significantly advance our knowledge of SWCNTs.

Introduction

The unique properties related to the quasi one-dimensional nature of single-wall carbon nanotubes (SWCNTs) give rise to great potential in numerous applications and have stimulated an ever-growing interest in both basic and applied research. Thus, the characterization and investigation of their fundamental and application oriented properties are a crucial prerequisite for tomorrow's applications. The isotope-controlled synthesis of SWCNTs provides a powerful means with which one can experimentally clearly identify and assign electronic and vibronic properties. Examples of observed and predicted phenomena include the presence of van Hove singularities in the electronic density of states, superconductivity,[1] the Tomonaga−Luttinger liquid behavior,[2,3] and the Peierls transition.[4,5] In addition, ^{13}C enrichment enables nuclear magnetic resonance (NMR) spectroscopy on SWCNTs that has proven to be a sensitive probe of the electronic structure of carbonaceous materials.[6] NMR is a widely used method in various fields ranging from physics to bioengineering and medicine. However, many studies are hampered by unwanted magnetic contaminants. Hence, SWCNT samples devoid of foreign magnetic contributions are an additional requirement for NMR studies. In addition SWCNT samples with well-defined and controllable narrow diameter distributions and high yield are also highly desirable for such experiments. High-yield catalyst-free SWCNTs can be produced via chemical vapor deposition (CVD) techniques[7] but suffer from limited diameter control and broad diameter distributions. This restricts their use in certain applications, for example, their use in functionalized SWCNTs via encapsulation techniques. Arc-discharge-synthesized SWCNTs can provide a narrower diameter distribution as compared to CVD but are less well defined than those obtained in laser evaporation. Furthermore, arc-discharge SWCNT samples contain greater numbers of byproducts, less diameter control, and lower yield than laser-evaporated SWCNTs. Laser-evaporated SWCNTs with readily controllable and well-defined narrow diameter distributions (and high yield) are the preferred choice for functionalization via encapsulation of molecules[8,9] and many other studies. In these studies, we show that all of the above-discussed requirements are met through our optimized laser-evaporated SWCNT synthesis route. The as-produced SWCNTs do not need any further aggressive purification to eliminate magnetic contaminations. This is highly encouraging for electron spin spectroscopy (ESR) and ^{13}C NMR studies on SWCNTs.[10,11] To our knowledge, no systematic study on the structural and electronic properties in controllable ^{13}C-enriched SWCNTs has been presented so far. In addition, the growth parameters were investigated in great detail. Novel changes in the synthesis conditions due to various isotope effects are also presented. The obtained uniform large-diameter ^{13}C-enriched SWCNTs are highly suited for filling and exploring novel one-dimensional phases in their interior[12−14] with the added advantage that spectroscopic responses from the SWCNTs and filling can be clearly separated by choosing the level of ^{13}C enrichment. Furthermore, their lack of any magnetic contribution makes them ideal SWCNTs for use in NMR-based studies and the quest to determine if SWCNTs exhibit superconductivity. In addition, their capacity to encapsulate molecular magnets (e.g., Mn12 acetate) and elements will, for example, enable coupling of spins to Luttinger liquids and novel Kondo-like physics to be explored. Such studies in spin and charge functionalities will undeniably lead to the discovery of new quantum phenomena.

* Corresponding author. E-mail: m.ruemmeli@ifw-dresden.de.
† IFW Dresden.
‡ Dresden University of Technology.
§ Budapest University of Technology and Economics.
|| Vienna University.

10.1021/jp066798b CCC: $37.00 © 2007 American Chemical Society
Published on Web 02/24/2007

Experimental Section

The SWCNTs were synthesized using a furnace-based pulsed laser evaporation method. The setup is very similar to that described previously,[15−17] with the only difference being that in this case the outer and inner (to restrict the reaction volume) tubes are made from alumina because the oven can reach temperatures as high as 1600 °C. In the present study, temperatures between 1200 and 1600 °C were used for the synthesis of the SWCNTs. A Q-switched high-power Nd:YAG laser (2.5 GW per pulse, pulse width = 8 ns) was used to evaporate catalyst-containing graphite targets using very-high-purity materials with nominal amounts of ^{13}C added (99% ^{13}C-enriched amorphous carbon from Sigma-Aldrich). Targets containing ratios of ^{12}C and ^{13}C ranging from natural ^{13}C content to near pure ^{13}C (99%) were prepared. The catalysts used were Pt with different proportions of Rh, Re, Cr, and Lu. Typically, the total catalyst content was 23% mass of the graphite targets. The evaporated products were then swept away by the carrier gas to a water-cooled copper cold finger behind the target, which provides a well-defined reaction stop point. All experiments were performed under atmospheric pressure, and the flow rates were varied between 0.2 L/min and 2.0 L/min. The reference SWCNTs (Nanocarblab, Russia) for the magnetic studies were synthesized via arc-discharge. The material was purified by the manufacturer and has a mean diameter of 1.40 nm as determined by multilaser Raman measurements.

Optical absorption spectroscopy (OAS) measurements were conducted with the product dispersed in acetone in an ultrasonic bath and dropped onto a KBr single crystal, giving a thin homogeneous film. A Bruker IFS 113V/88 spectrometer was used to obtain the optical absorption spectrum in the energy range of 0.35−2.35 eV, with a spectral resolution of 0.25 meV. For transmission electron microscopy, these films were floated off the KBr crystal, in water, and collected on standard Cu TEM grids (TEM, FEI Tecnai F30). Raman measurements were performed on a Bruker IFS100 Fourier transform Raman spectrometer and on a Dilor xy triple monochromator spectrometer.

To measure the local magnetic fields using electron spin resonance (ESR), the as-produced and reference SWCNTs were filled with $N@C_{60}$:C_{60}. The endohedral fullerene/fullerene solid mixture was prepared via a N_2 arc-discharge as described in ref 18. The fullerene encapsulation procedure was based on a low-temperature solvent method similar to that in ref 19. The SWCNTs were added to 1 mg/1 mL fullerene−toluene solutions and sonicated for 1 h. The resulting material was filtered from the solvent and then resuspended in excess toluene to remove nonencapsulated fullerenes and then refiltered. Raman spectroscopy at 488 nm laser excitation was used to check the material as described in ref 20. The peapods and unfilled SWCNTs were mixed with ESR silent high-purity SnO_2 in a mortar to separate the pieces of the conducting bucky paper. The samples were sealed under vacuum (<1 E^{-6} mbar). A Bruker Elexsys X-band was used for the ESR measurements with a typical microwave power of 10 mW and 0.01 mT magnetic field modulation at ambient temperature.

Results

Laser Ablation Synthesis. The potential of Pt and Rh as nonmagnetic catalysts has been shown previously.[21,22] We explored various combinations of these catalysts with other nonmagnetic catalysts (Rh, Re, Cr, and Lu), which are also suited to high temperature. Previous studies[23,24] have shown that multiple catalysts lead to an improved yield of SWCNT. When adding an assortment of mixed catalysts in different ratios, we found an optimum relative purity (quantity of SWCNT relative to all carbon species in the produced soot), with 14.0% Rh and 3.5% Re mass added to the Pt catalyst material. Although the purity of the SWCNT showed no significant dependence on the gas type, the yield (total amount of produced soot) was dependent on the carrier gas. Several gases (Ar, N_2, and Ar + 5% H_2) were evaluated. Slightly larger diameters were obtained with argon; however, the yield was better with N_2 in agreement with systematic studies on carrier gas and yield by Nishide et al.[25] The addition of H_2 to argon leads to a mean diameter reduction to levels below those obtained with N_2 and also leads to a broader diameter distribution. In addition, the amount of soot obtained was reduced relative to pure Ar. The great influence of the carrier gas highlights the complex dynamics of the formation of SWCNTs in the rapidly cooling evaporation cloud. The effects are most likely linked to changes in thermal conductivity and diffusion rates. The observed diameter distribution broadening upon adding H_2 is in agreement with earlier studies.[26] Additionally, we explored different flow rates (between 2 and 0.2 L/min) and found the optimum with regard to yield and purity to be 0.4 L/min Generally, the SWCNT mean diameter increases linearly with temperature.[27,12] However, those studies only investigated temperatures up to 1200 °C. In our studies, for the first time, we investigated temperatures up to 1600 °C. Our studies show that this linear increase in mean diameter with increasing temperature no longer holds above 1400 °C. The diameter versus temperature lines are flattened off for all investigated carrier gases and eventually become constant. This saturation in mean diameter dependence on temperature behavior is a novel experimental finding and very advantageous because the diameter dependence in the region of 1400−1600 °C is stable. Hence, the syntheses of SWCNTs in this region are not susceptible to thermal gradients. The relative purity can be determined from the ratio of the intensity of the first transition between van Hove singularities from semiconducting SWCNTs to the background intensity from optical absorption spectroscopy (OAS) because the spectrum reflects the difference in electronic states between SWCNTs and amorphous carbon.[28] The relative purity shows a temperature dependence that fits a Gaussian profile as illustrated in Figure 1 (inset). The optimum purity yield is obtained just above 1400 °C and shows a slightly better purity (>70%) as compared to a high-yield as-produced laser-evaporated SWCNT sample using Ni and Co catalysts with a known purity of 70%.[29]

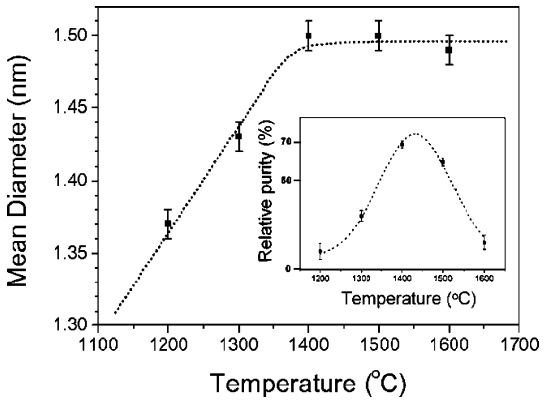

Figure 1. Mean diameter dependence on oven temperature for natural carbon SWCNTs. The dotted line is to guide the eye. Inset*:* Relative purity for as-produced soot vs oven temperature. The dotted line is a Gaussian fit.

Thus, the optimized set of parameters for a high and pure yield with a narrow diameter distribution (fwhm −0.2 nm) of

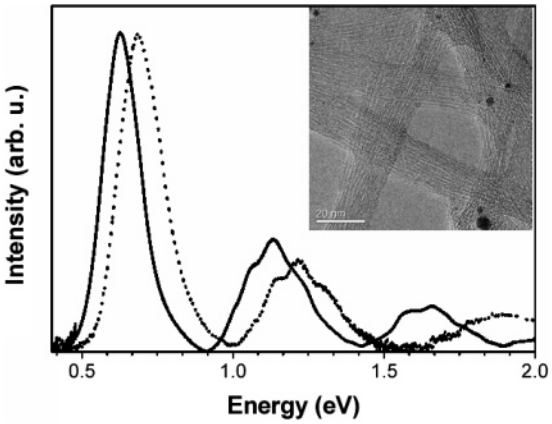

Figure 2. OAS spectra after strapping the background. Solid line, SWCNTs with natural ^{13}C content; dotted line, SWCNTs with 50% ^{13}C enrichment. N.B.: The spectral shift in peak positions is due to a shift in diameters and not ^{13}C enrichment. Inset*:* Typical TEM image of ^{13}C-enriched SWCNTs.

large-diameter SWCNTs ($d = 1.5$ nm) are obtained using a 82.5%/14.0%/3.5% Pt/Rh/Re catalyst mix at 1400 °C in 0.4 L/min N_2. Unless otherwise stated, these parameters are used throughout.

Spectroscopic Studies. Optical absorption spectroscopy (OAS) is a well-established means to determine the mean diameter and diameter distribution of SWCNTs.[9,30] We determined the mean diameter according to previously described methods[15] using the first semiconducting absorption peak, which has been shown to be representative of the diameter distribution and mean for all SWCNTs in a sample.[30] The OAS spectra showed a reduction in the mean diameter with ^{13}C enrichment. This is highlighted by the OAS spectra in Figure 2 from samples with a natural ^{13}C content and a high content of ^{13}C (50% as derived by Raman spectroscopy, described below). High-yield SWCNTs are obtained as illustrated in the transmission electron micrograph (TEM) inset image. A more detailed study of the mean diameters with the ^{13}C enrichment showed a parabolic dependence with a minimum diameter (ca. 1.3 nm) for a ^{12}C to ^{13}C ratio of 1:1 as illustrated in Figure 3a. Superimposed to that parabolic behavior, there is a general decrease of mean diameters with increasing ^{13}C content. The overall gradual decrease in mean diameter can be linked to a lowering of the metal carbon eutectic point due to the change in isotope weighting. The parabolic behavior centered at 50% points toward an isotope mixing effect. These are well known to have significant effects on phonon-mediated heat transport[31−33] and therefore, in our case, on the actual nucleation and growth temperature window of the CNT. Indeed, we find that increasing the furnace temperature can restore the ^{13}C-induced decrease of mean diameter. This clearly proves that ^{13}C is actually lowering the effective growth temperature. The restorations of the mean diameters with a higher furnace temperature of 1600 °C are also depicted in Figure 3a. An aspect of this isotope mixing effect is that the ^{13}C enrichment provides a novel route with which to tune the mean diameter of the SWCNT. Raman studies (discussed below) show that the ^{13}C enrichment of the SWCNT differs from that in the target prior to laser ablation, indicating fractionalization of the C isotopes. The difference between the starting target ^{13}C content and that of the obtained SWCNT shows a parabolic behavior as shown in Figure 3b. This rather strong fractionalization (in one single step) can be attributed to several processes. The evaporation of the target is more efficient for ^{12}C, and differential C species gas-phase transport can arise due to mass differences. The latter effect is considered minor.[34] In addition, there are differences in the diffusion rates (which are mass-dependent) of the C species within the molten catalyst particles. This effect is particularly noticeable during precipitation from a liquid.[35] All of these effects promote the lighter ^{12}C.

Raman spectroscopy is a widely used method to characterize SWCNTs. The line shape of the radial breathing mode (RBM) is very sensitive to the diameter distribution[36] because it scales as the inverse diameter of the SWCNTs. The effect of ^{13}C is a downshifting of all phonon energies due to the increased mass. Additionally, the random distribution of the isotopes leads to an increased line width.[37] Raman spectra of the diameter-dispersive RBM as well as the defect-induced (D line 1270 cm^{-1}) and graphitic line (G line 1550−1600 cm^{-1}) are depicted in Figure 4a and b, respectively. The good D/G ratio in Figure 4a indicates a low defect concentration for all levels of ^{13}C enrichment. The ^{13}C downscales all phonons according to $\omega/\omega_0 = \sqrt{(12+c_0)/(12+c)}$, where ω and c denote the phonon energy and ^{13}C concentration in the enriched material and ω_0 and $c_0 = 0.011$ of natural material, respectively.[37] Thus, the downscaling of the G line is a reliable means to determine the ^{13}C concentrations in the as-produced SWCNTs and targets.

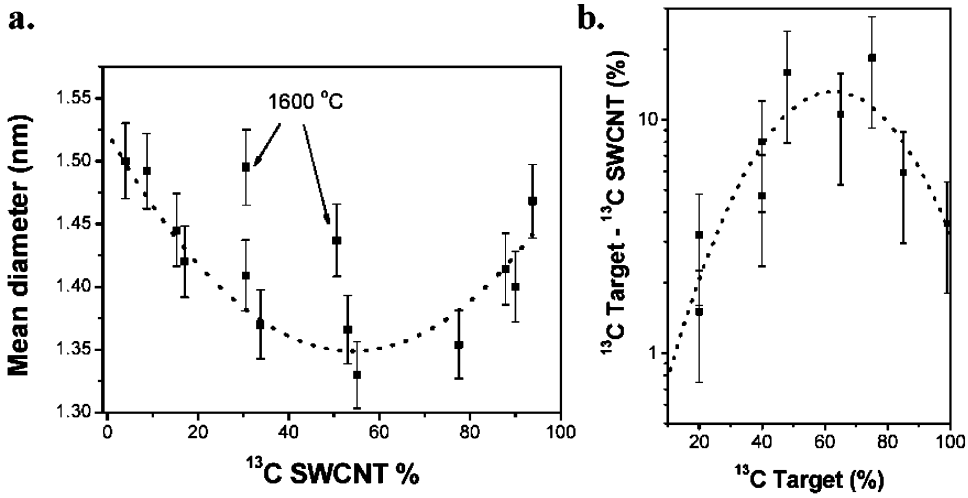

Figure 3. (a) Mean diameter variation with ^{13}C enrichment of SWCNTs synthesized at 1400 °C (the dotted line is to guide the eye); arrows, increase of mean diameters at 1600 °C. (b) Difference between ^{13}C content in target and as-produced SWCNTs (the dotted curve is to guide the eye).

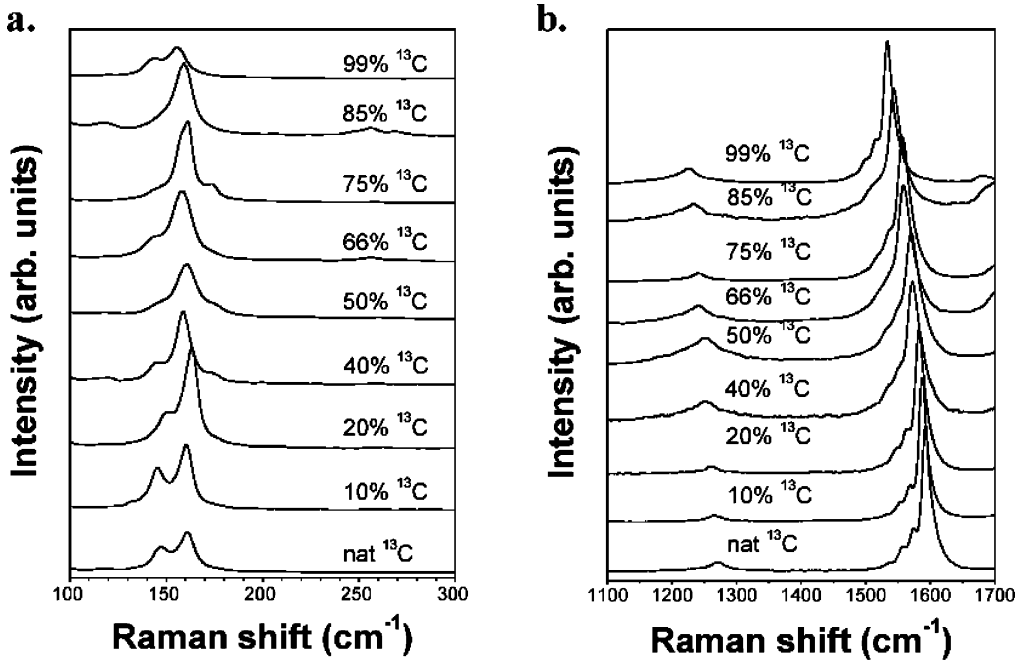

Figure 4. (a) Fourier transform Raman spectra (1064 nm) of RBM of SWCNTs with different ^{13}C contents. (b) Fourier Raman spectra (1064 nm) of the D and G lines of SWCNTs with different ^{13}C contents. The actual content was derived from the fitted Raman shift of the dominant peak in the G line. The spectra are normalized to G line intensity.

The individual components of the G line are clearly broadened because the fine structures get smeared out upon adding more ^{13}C up to around 50%; thereafter, the fine structure reappears. As a consequence of the previously discussed changes in mean diameter, the central position and the line profile of the RBM are modified, as shown clearly in ref 36. These changes in central position are of the same order of magnitude as those from ^{13}C enrichment. Although the changes in the shape of the RBM can be attributed to the altered mean diameters, the observed general downshift originates from ^{13}C enrichment and the altered mean diameters. An increase in line width of the RBM of very narrow SWCNTs has been reported before in ref 37 using high-resolution Raman spectroscopy. In this study, isotope-mixing-induced broadening is not observed. This is because the RBM of the larger diameter of our SWCNTs are not resolved into distinct lines for each diameter, and the total observed line width is then dominated by the spectral spread of the diameter distribution and not by the individual width of each constituent. The downscaling of phonon energy results in individual RBMs moving closer together, thus reducing the spectral spread. This counters the broadening of the individual lines.

Magnetic Studies. Electron spin resonance (ESR) allows one to determine the relative magnetism of multiple samples with ease, whereas absolute values are much harder to accomplish. In this study, we compare a highly purified SWCNT reference sample in which Ni and Y were used as the catalyst to our as-produced SWCNT with natural ^{13}C content. Local probe measurements were performed using N@C_{60} as a local spin probe (N@C_{60} encapsulated within the SWCNT). In Figure 5a, the ESR signals for both the reference sample and our as-produced SWCNT are shown. The broad signal observed for the reference sample with ΔH_{pp}= 60 mT originates from paramagnetic or superparamagnetic catalyst particles. This signal from the highly purified reference sample exhibits a signal similar to that from other SWCNT samples.[38,39] In stark contrast, the ESR signal from our as-produced SWCNT has a diminutive signal. The doubly integrated ESR signal, which is directly

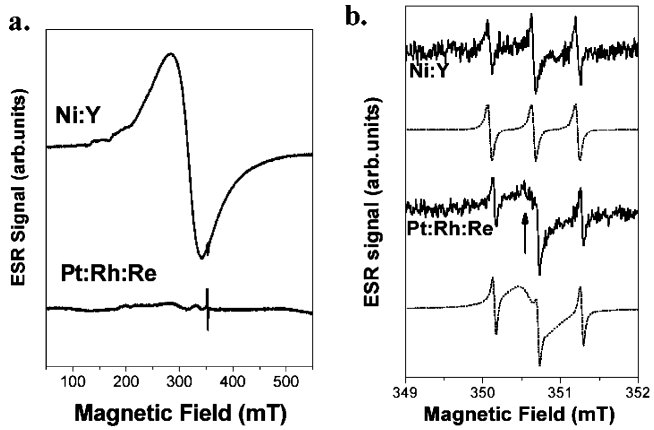

Figure 5. (a) Comparison of the residual magnetic particle content from the reference and as-produced SWCNTs from ESR. Both spectra are normalized by the instrument-dependent parameters and are offset for clarity. For the as-produced (Pt:Rh:Re) SWCNTs, the microwave cavity background starts to be seen. (b) Local stray magnetic field measured for the reference and as-produced samples encapsulated with N@C_{60}:C_{60} using ESR. The fits (dashed lines) for the triplet signals with Lorentzian lines are presented below each of the actual signals (solid lines). Note: For the as-produced sample (Pt:Rh:Re), a component not corresponding to the N@C_{60} triplet signal arising from a weak background signal is indicated by the arrow.

proportional to the magnetization in the sample, is over 100 times smaller than that of the reference sample. The intrinsic magnetism of the as-produced sample is probably even lower because residual paramagnetic centers in the microwave cavity limit the minimum detectable signal. Studies of the as-produced samples in a superconducting quantum interference device (SQUID) showed no magnetic signal, confirming the above ESR studies.

In addition to measurements of the relative magnetization of the samples, ESR also allows one to investigate the magnetic fields sensed by a local probe. In Figure 5b, we compare the spectra of N@C_{60}:C_{60} for both samples. It consists of a triplet

structure characteristic of the hyperfine splitting from the most abundant ^{14}N nuclei with nuclear spin 1. The line width is the same for the three lines and is a measure of the magnitude of the local magnetic fields. Line-width analysis using Lorentzian lines for the reference and as-produced samples yields $\Delta H_{pp} = 0.056$ mT and $\Delta H_{pp} = 0.041$ mT, respectively. The ESR line width of $N@C_{60}:C_{60}$ is 0.01−0.02 mT depends on the experimental conditions when in their pure crystalline form, viz., not encapsulated.[40] Thus, additional line broadening can be attributed to the presence of magnetic catalytic particles. Despite quantitative analysis being difficult due to the uncertainty of the nonbroadened line width, the current data shows significantly smaller stray magnetic fields for the as-produced sample relative to the reference sample.

Discussion

Summarizing, we have established a stable synthesis route for very-pure large-diameter SWCNTs, which gives highly reproducible results because the diameters obtained in laser ablation are independent of the synthesis temperature above 1400 °C. In contrast to standard catalysts, the optimized Pt/Rh/Re catalysts utilized in this study do not give rise to any magnetic impurities. Following this route with ^{13}C-enriched targets enables controlled isotope labeling. The samples were characterized with TEM, ESR, OAS, and Raman spectroscopy. OAS and TEM reveal a low abundance of amorphous carbon. The OAS data show changes in the mean diameter. These changes are attributed to isotope mixing effects, which we show can be compensated for. Raman spectroscopy reveals an almost negligible defect concentration and offers a convenient way of monitoring the ^{13}C-enriched synthesis of SWCNTs. ESR studies show the macroscopic magnetization and the local magnetic fields to be significantly smaller for our as-produced SWCNTs as compared to a commercial highly purified sample. SQUID measurements confirm that no magnetic signal is obtained from the samples. The results show that these samples are attractive for crucial studies investigating the superconductivity of SWCNTs because such studies are usually hindered by residual magnetization from catalyst particles. In addition, they are highly suitable for magnetic studies such as NMR[41] and studies on filled or functionalized nanotubes. In these fields, the ability to tailor the diameters and the phonon energies of the SWCNT templates is a practical and useful way to obtain clear separation of the spectroscopic responses. The presented laser-evaporation SWCNT synthesis route is notable for providing well-defined and controllable narrow diameter distributions, custom ^{13}C enrichment, and high yield. The numerous tailoring options and quality of the SWCNTs make them extremely attractive to a variety of important experiments and applications, which are not fulfilled by other synthesis routes.

Acknowledgment. We thank the DFG PI 440/1. C.K. thanks the International Max Planck Research School "Dynamical Processes in Atoms, Molecules and Solids" for a fellowship. A.G. acknowledges a Schrödinger fellowship J2493 from the Fonds zur Förderung der wissenschaftlichen Forschung (FWF). F.S. acknowledges the Zoltán Magyary programme for support and also support by the EU projects MERG-CT-2005-022103 and the Hungarian State Grants (OTKA) No. TS049881, F61733, and NK60984. We are grateful to R. Hübel and S. Leger for technical assistance.

References and Notes

(1) Tang, Z. K.; Zhang, L. Y.; Wang, N.; Zhang, X. X.; Wen, G. H.; Li, G. D.; Wang, J. N.; Chan, C. T.; Sheng, P. *Science* **2002**, *292*, 2462.

(2) Ishii, H.; Kataura, H.; Shiozawa, H.; Yoshioka, H.; Otsubo, H.; Takayama, Y.; Miyahara, T.; Suzuki, S.; Achiba, Y.; Nakatake, M.; Narimura, T.; Higashiguchi, M.; Shimada, K.; Namatame, H.; Taniguchi, M. *Nature* **2003**, *426*, 540.

(3) Rauf, H.; Pichler, T.; Knupfer, M.; Fink, J.; Kataura, H. *Phys. Rev. Lett.* **2004**, *93*, 096805.

(4) Bohnen, K. P.; Heid, R.; Liu, H. J.; Chan, C. T. *Phys. Rev. Lett.* **2004**, *93*, 245501.

(5) Connetable, D.; Rignanese, G.-M.; Charlier, J. C.; Blasé, X. *Phys. Rev. Lett.* **2005**, *94*, 015503.

(6) Pennington, C. H.; Stenger, V. A. *Rev. Mod. Phys.* **1996**, *68*, 855.

(7) Hata, K.; Futaba, D. N.; Mizuno, K.; Namai, T.; Yumura, M.; Ijima, S. *Science* **2004**, *306*, 1362.

(8) Takenobu, T.; Takano, T.; Shiraishi, M.; Murakami, Y.; Ata, M.; Kataura, H.; Achiba, Y.; Iwasa, Y. *Nat. Mater.* **2003**, *2*, 683.

(9) Yanagi, K.; Miyata, Y.; Kataura, H. *Adv. Mater.* **2006**, *18*, 437.

(10) Goze-Bac, C.; Latil, S.; Lauginie, P.; Jourdain, V.; Conard, J.; Duclaux, L.; Rubio, A.; Bernier, P. *Carbon* **2002**, *40*, 1825.

(11) Tang, X. P.; Kleinhammes, A.; Shimoda, H.; Fleming, L.; Bennoune, K. Y.; Sinha, S.; Bower, C.; Zhou, O.; Wu, Y. *Science* **2000**, *288*, 492.

(12) Meyer, R. *Science* **2004**, *289*, 1324.

(13) Smith, B.; Monthioux, M.; Luzzi, D. *Nature* **1998**, *396*, 323.

(14) Khlobystov, A.; Britz, D.; Ardavan, A.; Briggs, G. *Phys. Rev. Lett.* **2004**, *92*, 245507.

(15) Rümmeli, M. H.; Borowiak-Palen, E.; Gemming, T.; Pichler, T.; Knupfer, M.; Kalbác, M.; Dunsch, L.; Jost, O.; Silva, S. R. P.; Pompe, W.; Büchner, B. *Nano Lett.* **2005**, *5*, 1209.

(16) Jost, O.; Gorbunov, A.; Liu, X.; Pompe, W.; Fink, J. *J. Nanosci. Nanotechnol.* **2004**, *4*, 1.

(17) Jost, O.; Gorbunov, A. A.; Möller, J.; Pompe, W.; Liu, X.; Georgi, P.; Dunsch, L.; Golden, M. S.; Fink, J. *J. Phys. Chem. B* **2002**, *106*, 2875.

(18) Pietzak, B.; Waiblinger, M.; Murphy, T. A.; Weidinger, A.; Höhne, M.; Dietel, E.; Hirsch, A. *Chem. Phys. Lett.* **1997**, *279*, 259.

(19) Simon, F.; Kuzmany, H.; Rauf, H.; Pichler, T.; Bernardi, J.; Peterlik, H.; Korecz, L.; Fulop, F.; Janossy, A. *Chem. Phys. Lett.* **2004**, *383*, 362.

(20) Pichler, T.; Kuzmany, H.; Kataura, H.; Achiba, Y. *Phys. Rev. Lett.* **2001**, *87*, 267401.

(21) Saito, Y.; Tani, Y.; Miyagawa, N.; Mitsushima, K.; Kasuya, A.; Nishina, Y. *Chem. Phys. Lett.* **1998**, *294*, 593.

(22) Kataura, H.; Kumazawa, Y.; Maniwa, Y.; Ohtsuka, Y.; Sen, R.; Suzuki, S.; Achiba, Y. *Carbon* **2000**, *38*, 1691.

(23) Guo, T.; Nikolaev, P.; Thess, A.; Colbert, D. T.; Smalley, R. E. *Chem. Phys. Lett.* **1995**, *243*, 49.

(24) Lambert, J. M.; Ajayan, P. M.; Bernier, P.; Planeix, J. M.; Brotons, V.; Coq, B.; Castaing, J. *Chem. Phys. Lett.* **1994**, *226*, 364.

(25) Nishide, D.; Kataura, H.; Suzuki, S.; Tsukagoshi, K.; Aoyagi, Y.; Achiba, Y. *Chem. Phys. Lett.* **2003**, *372*, 45.

(26) Lebedkin, S.; Schweiss, P.; Renker, B.; Malik, S.; Hennrich, F.; Neumaier, M.; Stoermer, C.; Kappes, M. M. *Carbon* **2002**, *40*, 417.

(27) Bandow, S.; Asaka, S.; Saito, Y.; Rao, A. M.; Grigorian, L.; Richter, E.; Eklund, P. C. *Phys. Rev. Lett.* **1998**, *80*, 3779.

(28) Itkis, M. E.; Perea, D. E.; Jung, R.; Niyogi, S.; Haddon, R. C. *J. Am. Chem. Soc.* **2005**, *127*, 3439.

(29) Borowiak-Palen, E.; Pichler, T.; Liu, X.; Knupfer, M.; Graff, A.; Jost, O.; Pompe, W.; Kalenczuk, R. J.; Fink, J. *Chem. Phys. Lett.* **2002**, *363*, 567.

(30) Liu, X.; Pichler, T.; Knupfer, M.; Golden, M. S.; Fink, J.; Kataura, H.; Achiba, Y. *Phys. Rev. B* **2002**, *66*, 045411.

(31) Biernacki, S. W. *Phys. Rev. B* **1997**, *56*, 11472.

(32) Maruyama, S.; Miyauchi Y.; Taniguchi Y. International Symposium on Micro-Mechanical Engineering, Tsukuba, 2003; pp 45−51.

(33) Capinski, W. S.; Maris, H. J.; Bauser, E.; Silier, I.; Asen-Palmer, M.; Ruf, T.; Cardona, M.; Gmelin, E. *Appl. Phys. Lett.* **1997**, *71*, 2109.

(34) Jackson, S. E.; Günther, D. *J. Anal. At. Spectrom.* **2003**, *18*, 205.

(35) Taylor, H. P.; Epstein, S. *Geol. Soc. Am. Bull.* **1962**, *73*, 461.

(36) Kuzmany, H.; Plank, W.; Hulman, M.; Kramberger, C.; Grüneis, A.; Pichler, T.; Peterlik, H.; Jataura, H.; Achiba, Y. *Eur. Phys. J. B* **2001**, *22*, 307.

(37) Simon F.; Kramberger, C.; Pfeiffer, R.; Kuzmany, H.; Zolyomi, V.; Kurti, J.; Singer, P. M.; Alloul, H. *Phys. Rev. Lett.* **2005**, *95*, 017401.

(38) Claye, A. S.; Nemes, N. M.; Jánossy, A.; Fischer, J. E. *Phys. Rev. B* **2000**, *62*, 4845.

(39) Salvetat, J.-P.; Fehér, T.; Huillier, C. L; Beuneu, F.; Forró, L. *Phys. Rev. B* **2005**, *72*, 075440.

(40) Almeida Murphy, T.; Pawlik, Th.; Weidinger, A.; Höhne, M; Alcala, R.; Spaeth, J.-M. *Phys. Rev. Lett.* **1996**, *77*, 1075.

(41) Singer, P. M.; Wzietek, P.; Alloul, H.; Simon, F.; Kuzmany, H. *Phys. Rev. Lett.* **2005**, *95*, 236403.